Applied Surface Science 360 (2016) 306–314

Contents lists available at ScienceDirect

Applied Surface Science

journal homepage: www.elsevier.com/locate/apsusc

Solid-material-based coupling efficiency analyzed with time-of-flight secondary ion mass spectrometry

Bastian Muenster[a], Alexander Welle[b], Barbara Ridder[a], Daniela Althuon[a], Jakob Striffler[a], Tobias C. Foertsch[a], Lothar Hahn[a], Richard Thelen[a], Volker Stadler[c], Alexander Nesterov-Mueller[a,*], Frank Breitling[a,**], Felix F. Loeffler[a,***]

[a] Institute of Microstructure Technology, Karlsruhe Institute of Technology, Hermann-von-Helmholtz-Platz 1, 76344 Eggenstein-Leopoldshafen, Germany
[b] Institute of Functional Interfaces and Karlsruhe Nano Micro Facility, Karlsruhe Institute of Technology, Hermann-von-Helmholtz-Platz 1, 76344 Eggenstein-Leopoldshafen, Germany
[c] PEPperPRINT GmbH, Rischerstrasse 12, 69123 Heidelberg, Germany

ARTICLE INFO

Article history:
Received 6 July 2015
Received in revised form 27 October 2015
Accepted 29 October 2015
Available online 2 November 2015

Keywords:
Secondary ion mass spectrometry
C_{60} depth profiling
Particle-based solid phase peptide synthesis
Functionalized PEGMA coated surfaces
High-density peptide arrays
Combinatorial laser fusing

ABSTRACT

The coupling behavior of a microparticle embedded amino acid active-ester into a Poly(ethylene glycol)methacrylate-film, synthesized onto a silicon wafer by a grafting from approach, is characterized using dynamic time-of-flight secondary ion mass spectrometry (ToF-SIMS) to analyze the 3d distribution of the amino acids in the polymer film. Besides standard solid phase peptide synthesis, employing solubilized amino acids in a solvent, we used solid polymer microparticles, incorporating the amino acids. These microparticles were especially designed for a new technique to produce high-density combinatorial peptide microarrays: upon heating, the particles become viscous, which releases the embedded amino acids to diffuse and couple to the surface. In the scope of the development of this new particle-based application, ToF-SIMS is used to analyze a complex chemically modified polymer surface layer. Due to depth profile measurements, it is possible to investigate the particle-based coupling reaction not only on the surface, but also into the depth of the PEGMA film.

1. Introduction

In 1992 Ronald Frank developed the SPOT-Technique, an automated approach for a full combinatorial peptide synthesis in the array format on a membrane support [1,2]. This procedure is based on the concept of the solid-phase peptide synthesis (SPPS), which was invented by Bruce Merrifield in 1963 [3]. Today, the SPOT-Technique (see Fig. 1a) or variants thereof are commercially applied by companies like e.g. INTAVIS Bioanalytical Instruments AG [4], JPT Peptide Technologies GmbH [5], and others [6–8]. The combinatorial diversity arising from the 20 different amino acids is the major challenge for *in situ* peptide array synthesis. Meanwhile several research groups have investigated and reported novel strategies for the production of high-density peptide arrays [9]. Lithographic approaches, combining photomasks with photo-labile protecting groups [10,11] or more advanced technologies using digitally controlled patterned illumination to generate acids for deprotection by photolytic reactions [12] represent applied synthesis pathways. In 2007 and 2008, two straightforward xerographic methods to produce high-density combinatorial peptide microarrays were presented [13,14]. These techniques use polymer-based, amino acid loaded microparticles, which are addressed to a functionalized, Poly(ethylene glycol) methacrylate-(PEGMA) coated support [15,16] by electromagnetic fields (see Fig. 1b). The microparticles' hull consists of a commercially available polymer that was developed for toner particles in xerographic applications [14]. Microparticles are produced by dissolving one type of amino acid derivative and the polymer matrix material in a solvent, which is then evaporated in a spray dryer. The resulting polymer microparticles embed the amino acid derivatives. This material forms a brittle solid at room temperature but turns viscous at elevated temperatures. The viscous polymer efficiently confines the material to very small reaction sites, but at the same time frees the embedded amino acid derivatives to diffuse and couple to the surface (see Fig. 1c). Custom-made xerography toner-batches, one for each of the 20 amino acids, were developed and characterized to produce peptide microarrays. Towards the

* Corresponding author. Tel.: +49 72160829253.
** Corresponding author. Tel.: +49 72160823859.
*** Corresponding author. Tel.: +49 72160825221.
E-mail addresses: alexander.nesterov-mueller@kit.edu (A. Nesterov-Mueller), frank.breitling@kit.edu (F. Breitling), felix.loeffler@kit.edu (F.F. Loeffler).

http://dx.doi.org/10.1016/j.apsusc.2015.10.223

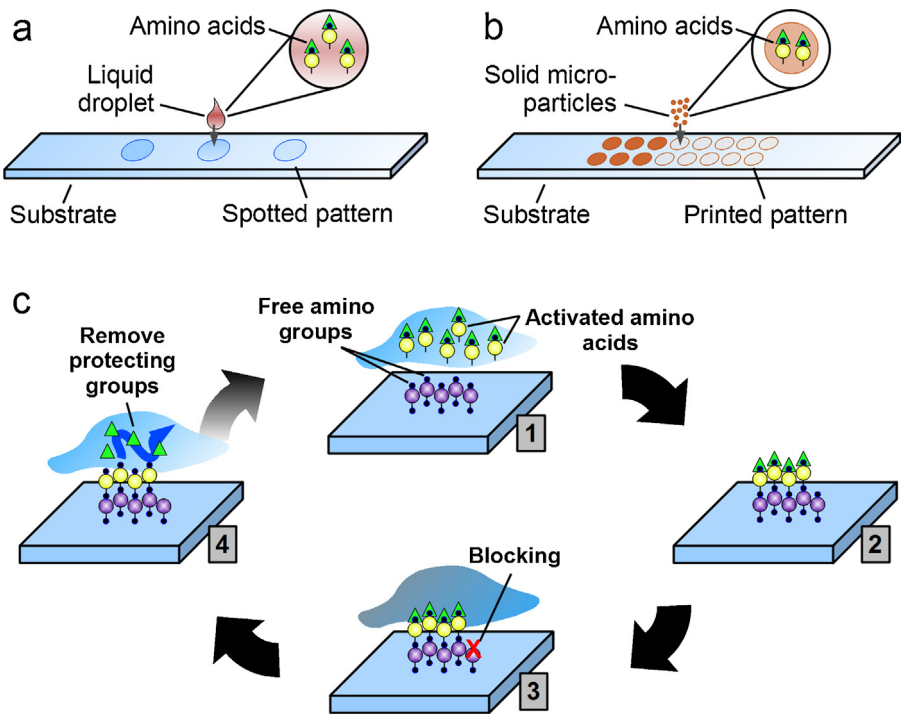

Fig. 1. Combinatorial synthesis of peptides. Amino acids are deposited on a surface with (a) the SPOT technology or (b) the particle-based technology. Activated amino acids in a solvent directly couple to the surface upon deposition, whereas solid microparticles have to be heated, to induce the coupling reaction. (c) The coupling reaction is performed in four steps: (1) deposition and (2) coupling of amino acids to amino groups, (3) blocking of unreacted amino groups and, (4) removing the amino-terminal protecting groups.

Table 1
Important aspects for SIMS molecular depth profiling.

Parameters and considerations	Applied system	Alternative approaches	Refs.
Sample			
Sputtering yield and damage creation	Poly(ethylene glycol)methacrylate exhibits a suitable balance of erosion and degradation of molecular structures due to sputter ion bombardment	Poly(lactide) and poly (methyl methacrylates) are suitable In contrast, Poly(styrene) undergoes cross-linking under irradiation and is intractable, see refs	[25], [27]
Low initial roughness	Spin coating layer, see text		
Homogeneity	Phase separated polymers would result in preferential sputtering and roughening of the sample during erosion		[28]
Instrumentation			
Sputter beam	Cs^+, 500 eV, no persistent molecular signals C_{60}^+, 20 keV, trityl signals detectable, see text	Small projectiles: Ar^+, Xe^+, O_2^+, Cs^+ rarely applicable: Rapid decay of molecular fragments Clusters: SF_5^+, Ar_x^+ provide often superior results	[29]
Analysis beam	Bi_3^+ field emission source, 25 keV, approx. 1 ns pulse width, high spectral resolution, and approx. 5 μm lateral resolution. Dose lower than 5% of sputtering dose to avoid extensive subsurface damage	C_{60}^+, single beam depth profiling with lower lateral resolution (20 μm), or long Bi pulses for improved lateral resolution (<500 nm)	[30]
Depth calibration	Performed by off-line profilometry at craters of different sputter beam fluences	In-line AFM analysis without air contact of the sample	[31]
Sample temperature	Room temperature	Cryogenic temperatures if necessary (possible cross linking can be reduced, providing constant erosion rates and good depth resolution)	[32]
Sample rotation	Fixed sample position allows for 3D imaging. Analysis beam and sputter beam from opposite directions, both 45° towards sample	Zalar rotation (not synchronized with data recording) for depth profiling of laterally homogeneous samples only. Improved depth resolution and sputtering yield was observed. Synchronized, 90° stepwise rotation	[30], [32], [33]

development of very high-density peptide arrays, Maerkle et al. successfully advanced this technology by combining the xerographic particle approach with advanced laser processing. This method, called Combinatorial Laser Fusing, allows for the synthesis of high-density peptide microarrays with a spot size of 10 μm [17,18].

Despite modern surface-sensitive spectroscopic techniques like IR- or XP-spectroscopy it is still challenging to analyze complex chemically modified thin films like the polymer coated silicon supports presented herein. We use ToF-SIMS as the method of choice to characterize the composition and the lateral distribution of characteristic moieties of our surfaces and thin films [19,20]. Today, the application range of ToF-SIMS includes engineering applications as well as the analysis of biological and organic samples [19,21–23]. While surface mapping of organic chemistries is usually readily achieved, molecular depth profiling and 3D imaging developed later [24] and gained strong attraction not before the development of polyatomic sputter ions like C_{60} and, more recently, Ar clusters, but still remain significant analytical challenge [25]. Table 1 lists the most important aspects of 3D imaging of organic layers based on dual beam depth profiling in SIMS. Apart from the applied technologies alternative approaches are given. It should be noted, that recently data of the detailed "VAMAS" multi-laboratory study were published: Layered samples of Irganox 1010 and either Irganox 1098 or Fmoc-pentafluoro-l-phenylalanine were used and analysis was performed using Ar cluster ion sputtering and either X-ray photoelectron spectroscopy (XPS) or ToF-SIMS [26].

2. Materials and methods

2.1. Materials

The chemicals and solvents used for the experiments were purchased from the following suppliers: 2,2′-Bipyridine (Bipy) (>99%), molar sieve (3 Å, 4 Å) from Alfa Aesar (Karlsruhe/Germany); Fmoc-β-alanine(-OH) from Iris Biotech (Marktredwitz/Germany); Chloroform (*pro analysi*, *p.a.*), Dichloromethane (DCM) (*p.a.*), *N*,*N*-Diisopropylethylamine (for synthesis), *N*,*N*′-Dimethylformamide (DMF) (*p.a.*), Hydrogen peroxide (H_2O_2) (30%) (for synthesis), Sulfuric acid (H_2SO_4) (for synthesis), Isopropyl alcohol (^{i}PrOH) (*p.a.*), Potassium hydroxide (KOH) (*p.a.*), Methanol (*p.a.*), Piperidin (for synthesis) from Merck (Darmstadt/Germany); (3-Amino)propyltriethoxysilane (APTES) (>99%), Copper(I) bromide (Cu(I)Br) (>98%), *N*,*N*′-Diisopropylcarbodiimide (>99%), Fmoc-Cys(Trt)-OPfp (>98%), 1-Methylimidazole (NMI) (>99%), α-Bromoisobutyryl-bromide (98%), Ethanol (>99.5%), Acetic anhydride (>98%) from Sigma Aldrich Chemie GmbH (Steinheim/Germany); S-LEC-P LT 7552 from Sekisui Chemical CO, LTD. (Osaka/Japan); graphite nanoparticles (99.9%, <30 nm, T_m = 3652 °C) from MIT Corp. (Richmond, CA/USA).

2.2. Microparticle production

8.8 g of the polymer matrix material S-LEC-P LT 75 52 (Sekisui/Japan) and 0.2 g graphite nanoparticles were dissolved/suspended in 100 ml dichloromethane (*p.a.*) by vigorous stirring. After the polymer was dissolved and the nanoparticles were homogeneously dispersed, 1.0 g of Fmoc-Cys(Trt)-OPfp was added and dissolved. The solution/dispersion was pumped into a B-290 spray-dryer (in combination with the B-295 Inert-Loop, which allows spray drying of organic solvents) over a silicon tube. The spray-dryer and the Inert-Loop were purchased from Büchi Labortechnik GmbH (Essen/Germany). After the spray drying process was completed, the resulting particles were taken from the collecting vessel.

2.3. Surfaces and solid supports

Silicon wafers served as solid supports. After 30 min of cleaning with 30% (v/v) hydrogen peroxide (30%) in concentrated sulfuric acid in a petri dish under constant shaking, the cleaning solution was carefully decanted and the surface was rinsed with Millipore water and ethanol (*p.a.*) and dried in an airstream.

Immediately after drying, the silicon wafer was covered with 10 ml of a solution of 290 μl (3-Amino) propyltriethoxysilane (APTES) and 240 μl Millipore water in ethanol (*p.a.*) and incubated for 16 h inside a desiccator under argon-atmosphere. The decanting of the APTES-solution has to be carried out under constant, thoroughly rinsing with ethanol (*p.a.*). A curing of the surface while rinsing, might lead to crystallization of non-reacted APTES traces that could damage the APTES-layer on the surface. Afterwards, the wafer was washed with ethanol (*p.a.*) (3 × 3 min) on a shaker, dried in an airstream and tempered in an oven at 120 °C for 45 min to complete the condensation reaction.

A 0.6 mM *N*,*N*-Diisopropylethylamine (DIPEA) solution in dry dichloromethane (DCM) (stored above 4 Å molar sieve) was provided in a Schlenk-flask under argon atmosphere and cooled down to 0 °C. Under vigorous stirring, a 0.2 mM α-Bromoisobutyryl bromide solution in dry DCM (stored above 4 Å molar sieve) was added via a dropping funnel under argon flow. The APTES-functionalized wafer was covered by the reaction mixture, placed inside a petri dish in the desiccator. After 16 h of incubation at room temperature under argon, the reaction solution was decanted and the surface was washed on a shaker with dry DCM (2 × 3 min) and methanol (*p.a.*) (2 × 2 min) and dried in an airstream.

All following steps were performed under argon flow. A solution of 10 ml PEGMA, 10 ml Millipore water and 10 ml methanol (*p.a.*) was set up inside a Schlenk-flask, which was evacuated three times and put under argon atmosphere before. 280 mg of 2,2′-Bipyridine (Bipy) were added to the solution and dissolved under stirring. After the Bipy was dissolved completely, 128 mg Cu(I)Br were added and the reaction mixture was stirred for another 5 min. The functionalized surface was incubated in the PEGMA solution inside a petri dish in the desiccator for 16 h under argon atmosphere at room temperature. After the incubation was complete, the surface was rinsed with Millipore water and washed with Millipore water (3 × 5 min) and methanol (2 × 3 min) on the shaker and dried in the airstream. In the case of remaining residua from the polymerization reaction, the surface was cleaned in chloroform by sonification (<30 s).

2.4. Fmoc-β-alanine functionalization of the PEGMA film

1.2 equivalents of *N*,*N*′-Diisopropyl–carbodiimide (DIC) were added to a 0.2 M solution of Fmoc-β-alanine in dry DMF (stored above 3 Å molar sieve) inside a Schlenk-flask under argon with a syringe via a septum. After stirring for 5 min at room temperature, 2.0 equivalents of 1-Methylimidazole (NMI) were added and the reaction mixture was stirred for another minute. The PEGMA film on top of the silicon wafer was covered with the DMF solution inside a petri dish, placed in a desiccator under argon flow. The closed desiccator has now been evacuated and filled with argon three times. The incubation was performed overnight, while coupling to hydroxyl-groups. Because of the higher nucleophilicity, 2 h of incubation was sufficient for coupling to amino-functions. After the coupling reaction was completed, the solid support was washed with DMF (*p.a.*) (3 × 5 min) and methanol (2 × 3 min) on a shaker, dried in an airstream and stored at 4 °C under argon until further use.

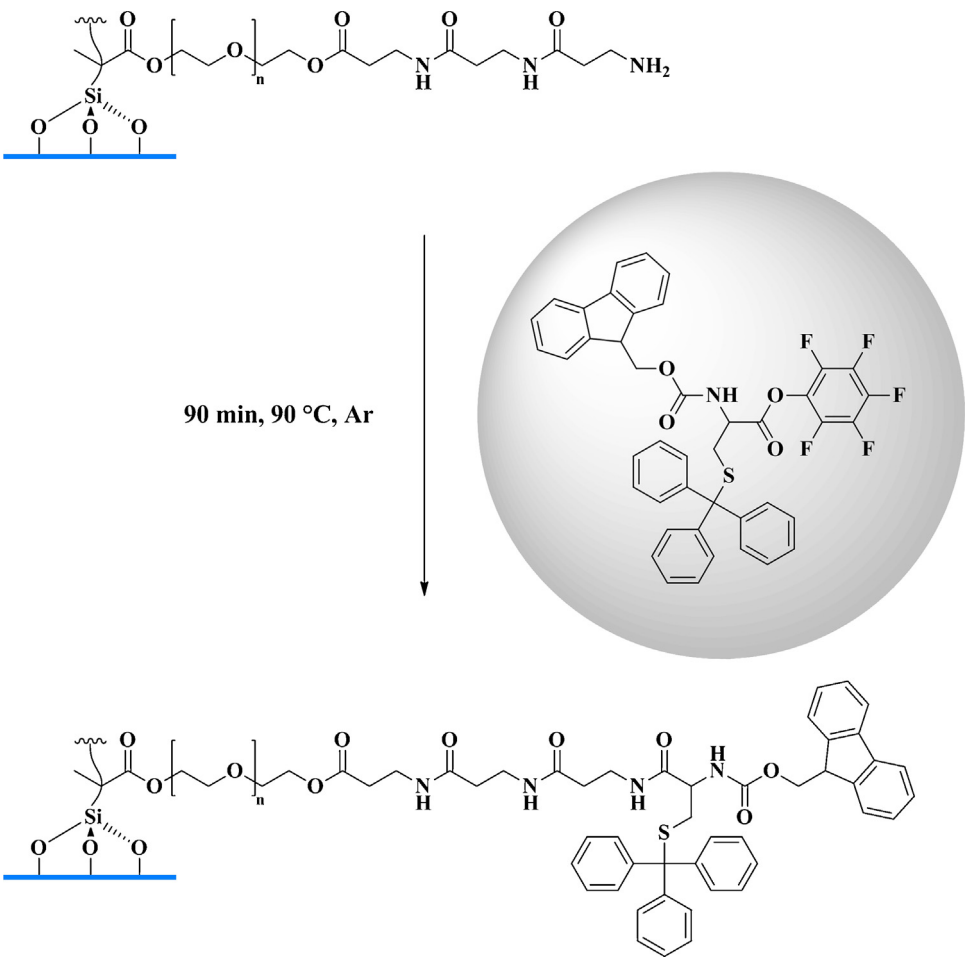

Fig. 2. Outline of the particle-based coupling reaction of Fmoc-Cys(Trt)-OPfp inside a PEGMA film. The PEGMA film was synthesized on the surface of a silicon wafer by a grafting from approach via si-ATRP and functionalized with three β-alanine spacer-molecules prior to the Fmoc-Cys(Trt)-OPfp immobilization.

Spray drying parameters		SEM image of the resulting particle batch
N_2-flow	60 L/min	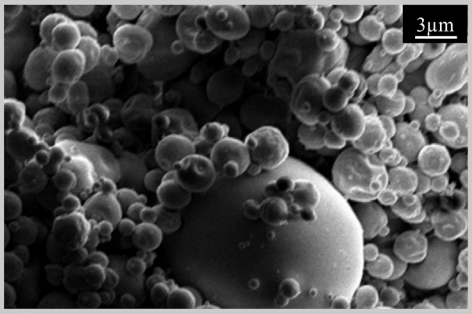
Temperature Inlet	70 °C	
Temperature Outlet	39 °C	
Aspirator	100 %	
Pump	20 %	
Nozzle Cleaner	2/min	

Fig. 3. Spray drying parameters used for microparticle production (left). SEM image, showing the Fmoc-Cys(Trt)-OPfp loaded microparticles (right).

2.5. Blocking

After each coupling reaction on the solid support, non-reacted functional groups were acetylated by covering the PEGMA film with a solution of 1 ml acetic anhydride, 2 ml DIPEA in 7 ml DMF (*p.a.*). After this the solid support was washed with DMF (*p.a.*) (3 × 5 min) and methanol (2 × 3 min) on a shaker, dried in an airstream and stored at 4 °C under argon until further use.

2.6. Removal of the Fmoc-protecting group

The Fmoc-protecting group was removed by covering the PEGMA film on the silicon wafer with a 20% (v/v) piperidine solution in DMF at room temperature for 20 min. Reaction yields of the Fmoc-β-alanine coupling steps were controlled by photometric determination of the concentration of the piperidyl-dibenzofulvene adduct inside the deprotection solution. After deprotection, the solid support was washed with DMF (*p.a.*) (3 × 5 min) and methanol (2 × 3 min) on a shaker, dried in an airstream and stored at 4 °C under argon until further use.

2.7. Particle-based coupling reaction

The microparticles were deposited on the synthesis surface (6.25 mg/cm^2) with a spatula. Subsequently, the surface was heated

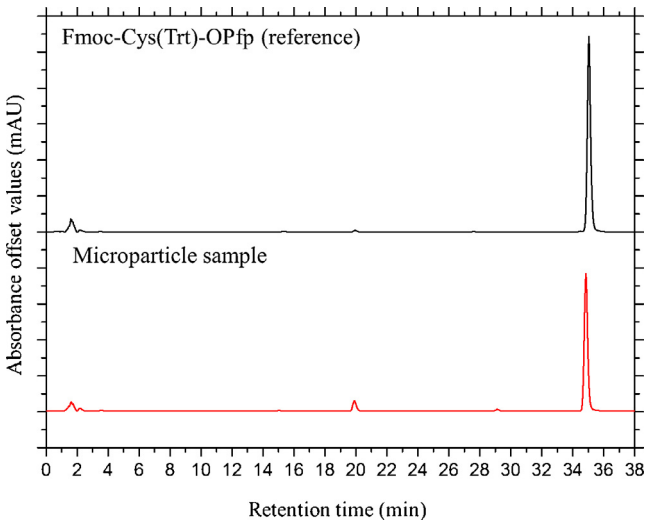

Fig. 4. Comparative HPLC measurements. The pure Fmoc-Cys(Trt)-OPfp reference (black), as well as the microparticle sample (red) showed a peak at a retention time of about 35 min. (For interpretation of the references to color in this figure legend, the reader is referred to the web version of the article.)

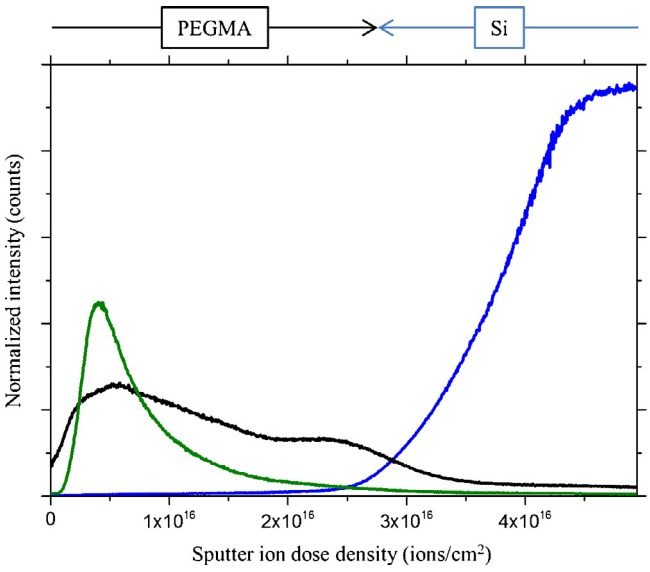

Fig. 5. ToF-SIMS depth profile of a PEGMA film, functionalized with three β-alanine spacer-molecules, synthesized on a silicon wafer, after particle-based coupling of Fmoc-Cys(Trt)-OPfp. Sputtering with a 0.5 keV Cs^+-source. Green: $^{79}Br^-$ -signal, black: $^{32}S^-$ -signal, blue: $^{28}Si^-$ -signal. All signals were normalized to the total ion counts. (For interpretation of the references to color in this figure legend, the reader is referred to the web version of the article.)

in a petri-dish in the oven for 90 min at 90 °C under argon. After the sample was cooled down to room temperature, non-reacted amino acid and other particle components remaining on the synthesis surface were quickly rinsed away with DCM (*p.a.*). Afterwards, the surface was washed with DCM (*p.a.*) (3 × 5 min) and methanol (*p.a.*) (2 × 3 min) in a petri-dish on a shaker and dried in an airstream.

2.8. Solution-based coupling reaction

The PEGMA film synthesized on top of a silicon wafer, functionalized with three β-alanine spacer-molecules was covered by a 0.2 M Fmoc-Cys(Trt)-OPfp solution in dry DMF (stored above 3 Å molar sieve) inside a petri-dish in a desiccator under argon flow. After 2 h of incubation at room temperature under argon, the PEGMA film was washed with DMF (*p.a.*) (3 × 5 min) and methanol

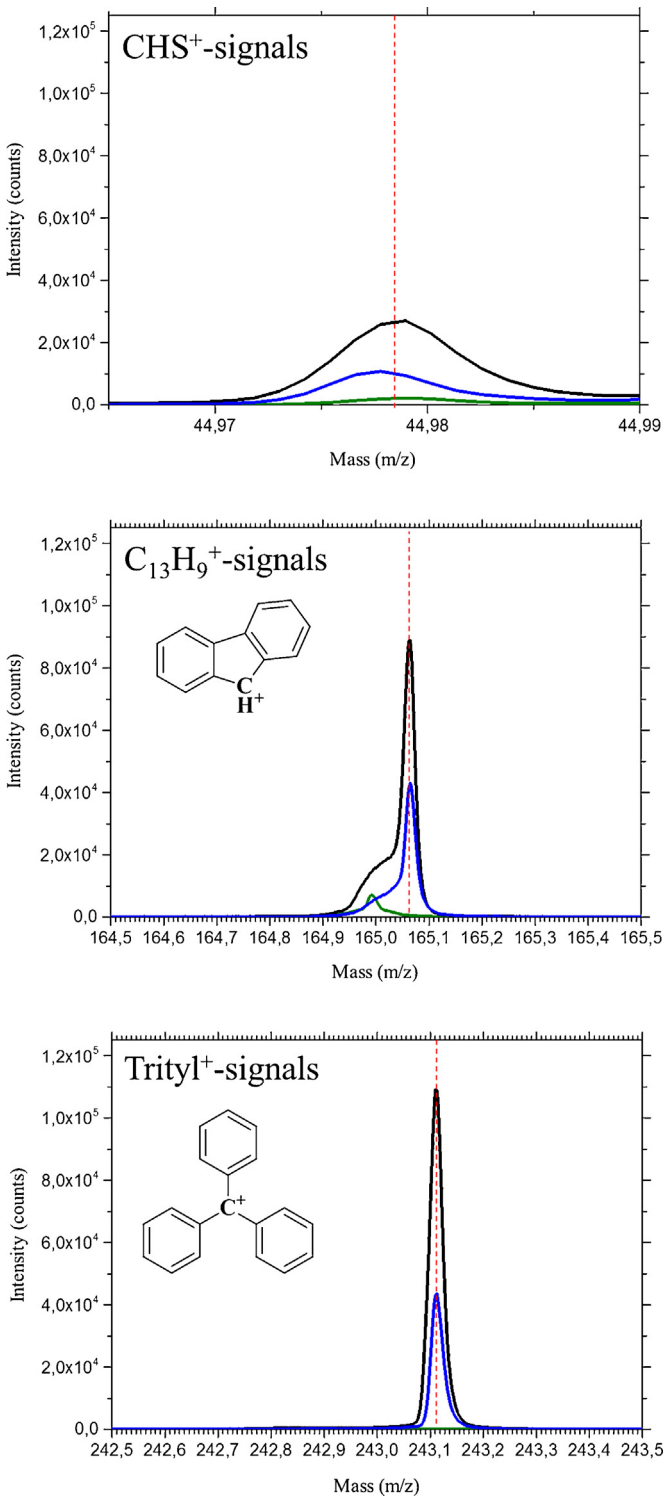

Fig. 6. Characteristic fragments taken from ToF-SIMS depth profile measurements of PEGMA films functionalized with three β-alanine spacer-molecules, synthesized on silicon wafers, before and after particle- and solution-based immobilization of Fmoc-Cys(Trt)-OPfp. Sputtering was done with 20 keV C_{60}^+-ions. All mass-signals were integrated over the complete depth of the corresponding depth profile measurements until reaching the Si substrate. Black: solution-based Fmoc-Cys(Trt)-OPfp immobilization, blue: particle-based Fmoc-Cys(Trt)-OPfp immobilization, green: functionalized PEGMA film before immobilization (blank reference). (For interpretation of the references to color in this figure legend, the reader is referred to the web version of the article.)

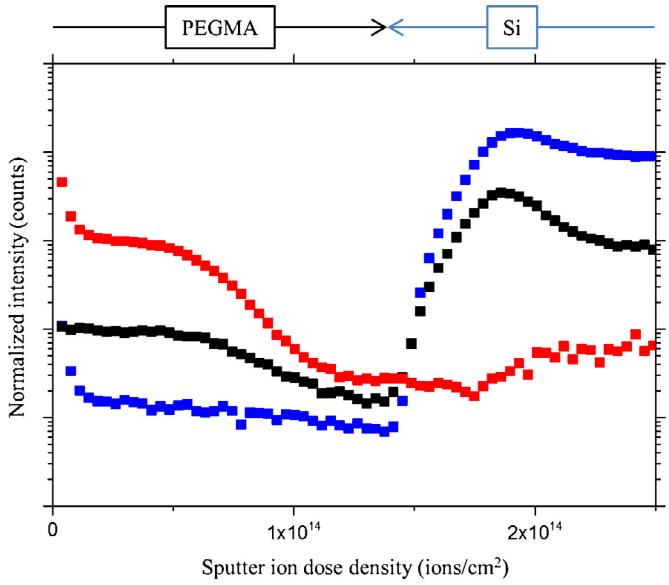

Fig. 7. ToF-SIMS depth profile of a 100% PEGMA film, functionalized with three β-alanine spacer-molecules, synthesized on a Si-wafer, after particle-based coupling of Fmoc-Cys(Trt)-OPfp. Sputtering with 20 keV C_{60}^+-ions. Red: Trityl$^+$-signal (m/z = 243.02), black: CHS$^+$-signal (44.98) overlapping the SiOH$^+$-signal, blue: $^{28}Si^+$-signal (27.98). (For interpretation of the references to color in this figure legend, the reader is referred to the web version of the article.)

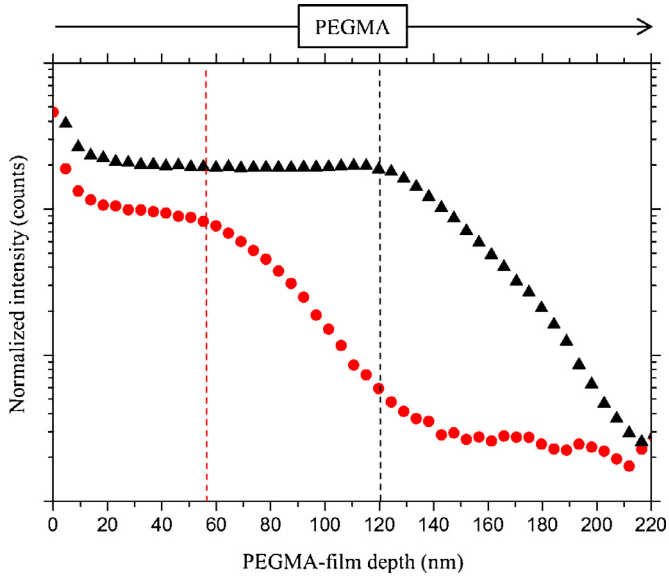

Fig. 8. Trityl$^+$ depth profiles of PEGMA films, functionalized with three β-alanine spacer-molecules, synthesized on silicon-wafers, after particle- *vs.* solution-based immobilization of Fmoc-Cys(Trt)-OPfp. Sputtering with 20 keV C_{60}^+-ions. Black: solution based Fmoc-Cys(Trt)-OPfp immobilization, red: particle-based Fmoc-Cys(Trt)-OPfp immobilization. (For interpretation of the references to color in this figure legend, the reader is referred to the web version of the article.)

(2 × 3 min) on a shaker, dried in an airstream and stored at 4 °C under argon until further use.

2.9. ToF-SIMS measurements

The ToF-SIMS measurements were performed on a TOF.SIMS5 device with a reflectron ToF-analyzer, ION-TOF GmbH (Münster/Germany). A Bi-Cluster Liquid Metal Ion Gun generated bunched Bi^+/Bi_3^+-primary ion pulses at 25 keV with 1.1–1.3 ns duration. When measuring in spatially resolved mode, the

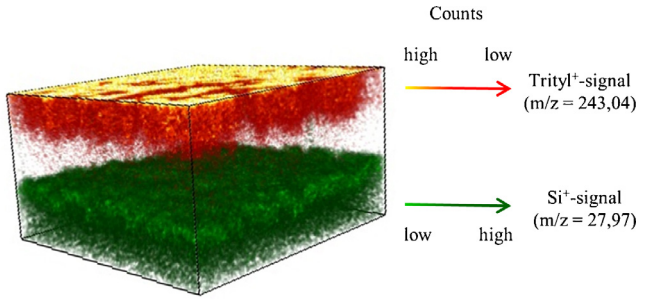

Fig. 9. 3d-rendering model based on the TOF-SIMS depth scan of a PEGMA film, functionalized with three β-alanine spacer-molecules, after particle-based immobilization of Fmoc-Cys(Trt)-OPfp. $x = y = 300$ μm, z axis not to scale.

instrument was able to scan a 500 × 500 μm^2 area with a lateral resolution of 4 μm. While measuring depth profiles, the surface was eroded by sputtering with 500 eV Cs^+ or 20 keV C_{60}^+ ions. The Cs gun was operated in interlaced mode, this means after each Bi pulse for mass spectrometry the Cs sputter beam was activated during each drift time of the secondary ions in the analyzer. The C_{60} gun was operated in non-interlaced mode, this means several frames were taken with Bi primary ions for analysis followed by a 1.4 s C_{60} erosion cycle and a 0.6 s pause for charge compensation. Surface charges were compensated by a 21 eV electron flood gun. C^+, CH^+, CH_2^+ and CH_3^+ as well as C^-, C_2^-, C_3^- signals were used for calibration.

2.10. SEM images

The scanning electron microscope (SEM) images were obtained using a Supra 60 VP scanning electron microscope from Carl Zeiss GmbH (Jena/Germany). Prior to the SEM imaging the samples were coated with a 15 nm silver layer by a K575X Sputter Coater from Quorum Technologies Ltd (East Sussex/UK) using a 30 μm Ag-target, sputtering 3.5 min with 25 mA.

2.11. HPLC measurements

The comparative HPLC measurement was performed on an ÄKTA^{TM} Purifier 10 from Amersham Pharmacia Biotech (Freiburg/Germany). The HPLC runs were carried out via a CC 125/3 Nukleosil 100-3 C18 HD column in combination with a CC 8/3 Nucleosil 100-3 C18 HD pre-column, both from Macherey–Nagel (Düren/Germany). A 0.05 M aqueous triethylammonium phosphate buffer (pH 2.25) served as Eluent A. Eluent B was a mixture of 10% (v/v) Eluent A in acetonitrile. The mobile phase was pumped with a flowrate of 0.5 ml/min and a gradient of 60–95% (v/v) referring to Eluent B in 30 min at 23 °C. The detection wavelength was 215 nm.

3. Results and discussion

For the experiments, a PEGMA film synthesized on top of a silicon wafer by surface-induced Atom Radical Transfer Polymerization (si-ATRP) served as solid support. To generate nucleophilic NH_2-groups inside the PEGMA film, the polymer was functionalized with three β-alanine spacer-molecules prior to the particle-based amino acid immobilization. To acquire a reliable ToF-SIMS depth profile, we introduced an amino acid derivative into the PEGMA film which yields strong and clearly assignable secondary ions, as outlined in Fig. 2.

The Fmoc-S-trityl-L-cysteine-pentafluorophenylester (Fmoc-Cys(Trt)-OPfp) was embedded into polymer microparticles by spray drying, using a B-290 Minispray-dryer in combination with

an Inert-Loop B-295 (Büchi Labortechnik GmbH, Essen/Germany). Dichloromethane was used to dissolve and disperse the particle components homogeneously prior to the spray drying process. To determine the particle size distribution, a MASTERSIZER 2000 from Malvern Instruments (Worcestershire/UK) was used. A particle batch with a diameter size distribution showing the characteristic values $d(0.1) = 0.8\ \mu m$, $d(0.5) = 3.4\ \mu m$ and $d(0.9) = 6.4\ \mu m$ was produced by applying the spray drying parameters from Fig. 3. Differential scanning calorimetry measurements revealed that the microparticles undergo a glass transition at $T_g = 65.6\ ^\circ C$, which is in accordance to the data published by Stadler et al. [14]. Comparative HPLC measurements validated the integrity of the Fmoc-Cys(Trt)-OPfp, embedded inside the microparticles (Fig. 4).

Equal amounts of particles were spread over comparably sized surfaces to produce samples for the ToF-SIMS measurements. The particle layers were heated at 90 °C under argon. Upon heating, the particle matrix material becomes viscous, converting into a gel-like state, and thus, mediates the coupling of the OPfp-activated cysteine derivative into the functionalized PEGMA film. After the particle-based coupling reaction, the solid support was washed thoroughly to remove non-reacted amino acid and remaining particle components from the polymer film. After drying the sample in an airstream, the ToF-SIMS measurements were performed.

First ToF-SIMS depth profiling results, obtained by using a 0.5 keV Cs^+ ion beam to sputter the surface and 25 keV Bi^+-ion pulses to analyze the secondary ions in interlaced mode, are shown in Fig. 5. The $^{79}Br^-$-signal of the sample is shown in green. Br^- can be found inside the functionalized polymer film on the silicon wafer, because the PEGMA film was synthesized by a grafting from si-ATRP approach. Serving as a starting point for the ATRP reaction, α-Bromo-isobutyrylbromid was coupled to an (3-Aminopropyl) triethoxysilane (APTES) layer, immobilized on the silicon wafer surface. The $^{79}Br^-$-signal shows an accumulation of Br^- in the upper region of the polymer film. A possible explanation for this concentration effect, considering the si-ATRP reaction mechanism, is the propagation of the PEGMA backbone which is associated with the bromide "growing out" of the polymer film [34–36].

Following a maximum, the $^{79}Br^-$-signal declines when reaching deeper regions of the polymer film. As soon as the sputter erosion removed the PEGMA film and reached the surface of the silicon wafer, the Si^--signal (Fig. 5, blue line) increases, while all other signals deplete. With the side chain of the cysteine derivative, a sulfur heteroatom was introduced into the PEGMA film by particle-based immobilization. The development of the S^--signal (Fig. 5, black line) was monitored by the ToF-SIMS depth profile. Immediately before the Si^--signal gains intensity the S^--signal shows a local maximum. This observation can be referred to the forward implantation of individual sulfur atoms into deeper regions of the bulk of the PEGMA coating during Cs^+-sputtering or changing matrix effects at the PEGMA/Si interface. The axis of abscissae represents a sputter ion fluence scale that cannot be directly converted into a depth scale. When sputtering two different material layers, as in our case (PEGMA film/silicon wafer), the linear correlation between sputter ion dose and depth of erosion is lost due to different sputter yields.

To reduce the forward implantation effects and the degradation of larger molecular structures ahead of the erosion front, a C_{60}^+ sputter beam was applied for molecular depth profiling. C_{60} is known to be less destructive during the sputter process [37–39]. The following investigation of a PEGMA film synthesized on a silicon wafer, functionalized with three β-alanine spacer-molecules, was performed before and after particle- and solution-based Fmoc-Cys(Trt)-OPfp immobilization. A blank PEGMA film with the spacer molecules served as reference. We compared the corresponding functionalized polymer film after coupling the Fmoc-Cys(Trt)-OPfp from solution with a similarly processed particle-based coupling sample. Solution-based immobilization was done by spreading a 0.2 M solution of Fmoc-Cys(Trt)-OPfp in *N,N′*-Dimethylformamide (DMF) over the polymer film on the silicon wafer at room temperature under argon, while the particle-based coupling reaction was performed as described above. After carefully washing and drying the samples, ToF-SIMS measurements were performed. The depth profiles (Fig. 6) showed characteristic signals, clearly assignable to molecule-ions originating from the immobilized Fmoc-Cys(Trt). Fig. 6 illustrates the CHS^+-signal ($m/z = 44.98$) generated from the cysteine derivative's side chain, the $C_{19}H_{15}^+$-signal ($m/z = 243.04$) derived from the trityl side chain protecting group, and the $C_{13}H_9^+$-signal ($m/z = 165.07$), attributed to the fragmentation of the N-terminal Fmoc-protecting group. For signals integrated over the whole depth of depth profile measurement, the highest intensities were always obtained from the sample prepared by solution-based Fmoc-Cys(Trt)-OPfp immobilization (Fig. 6, black lines).

Due to the nearly complete absence of other interfering signals (see green curves in Fig. 6), the $trityl^+$-signal appeared to be the best indicator for the characterization of the Fmoc-Cys(Trt)-OPfp immobilization inside the PEGMA film. Furthermore, the analysis of large (multi atomic) secondary ions eliminates forward implantation effects.

Fig. 7 shows the depth profile measurements on a functionalized PEGMA film after particle-based immobilization of Fmoc-Cys(Trt)-OPfp. This diagram shows the normalized intensities of the $trityl^+$-(Fig. 7, red data points), the CHS^+- (Fig. 7, black data points) and the Si^+-signal (Fig. 7, blue data points) plotted against the sputter ion dose density. As expected, the curve progression of the $trityl^+$-signal (Fig. 7, red data points) is in accordance with the CHS^+-signal (Fig. 7, black data points) before reaching the surface of the silicon wafer. However, when the silicon wafer surface is reached – which is indicated by the gradually increasing Si^+-signal (Fig. 7, blue data points) – the CHS^+-signal unexpectedly seems to gain intensity. This behavior is caused by the mass overlap of the wafer specific $SiOH^+$ ion ($m/z = 44.9802$) and the CHS^+ side chain fragment ($m/z = 44.9804$). However, the very low Si^+ intensities found for low erosion depths indicate the absence of this cross talk within the polymer layer.

To assess the penetration-depth of Fmoc-Cys(Trt)-OPfp within the functionalized PEGMA film, $trityl^+$-signals of the two samples, coupled from solution *vs.* coupled from viscous particle matrix material, were compared (Fig. 8). Immobilization of the cysteine derivative to the PEGMA film from solution and particle matrix was performed as described above. Fig. 8 shows the determined ToF-SIMS depth profiles. To convert the sputter ion fluence into a depth scale, the depths of several sputter craters with known C_{60} ion fluences were measured by profilometry directly after the ToF-SIMS experiment [23].

While the $trityl^+$-signal of the solution-based immobilization (Fig. 8, black data points) is constant to a penetration-depth of 120 nm, the $trityl^+$-signal of the particle-based coupling reaction (Fig. 8, red data points) already starts to decline at roughly 60 nm. This depth does not correspond to the total thickness of the PEGMA layer (compare Si signal in Fig. 6). These results can be explained by the different properties of the used solvents: while PEGMA films show a good swelling behavior in DMF (at room temperature), the sterically demanding polymer chains of the viscous particle matrix material do not penetrate into deeper regions of the polymer film to mediate the coupling reaction (at 90 °C). Fig. 9 shows the distribution of Fmoc-Cys(Trt) in the PEGMA film on the silicon wafer, employing particle-based coupling (see supplementary material Video). The 3d-rendering model is based on the mass spectrometric data, collected during a ToF-SIMS depth profile, showing the $trityl^+$- and Si^+-signals.

To rule out interference of material, which could be deposited on top of the polymer film, we acquired scanning electron microscope

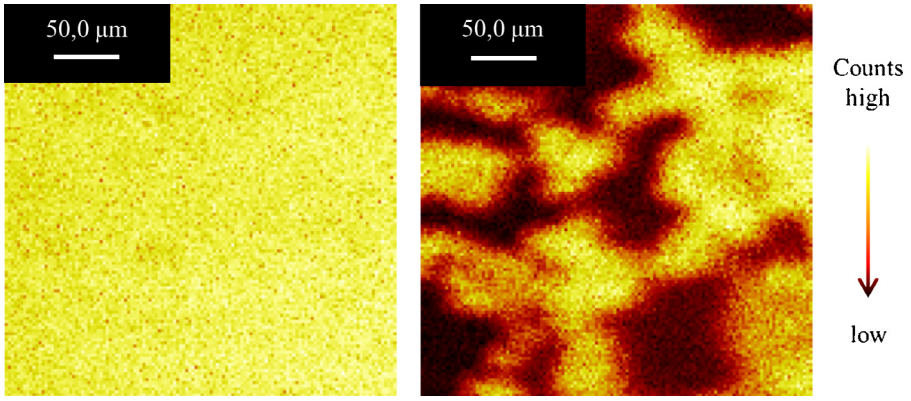

Fig. 10. Heat maps of the trityl$^+$-signal distributions obtained from ToF-SIMS measurement on PEGMA coated silicon wafer surfaces, functionalized with three β-alanine spacer-molecules after solution- (left) and particle- (right) based immobilization of Fmoc-Cys(Trt)-OPfp.

(SEM) images of the surface of the PEGMA film (see supplementary material Fig. S1) after particle-based immobilization and the corresponding washing steps. We thereby verified that no particle material remained on top of the sample, which might have distorted the model shown in Fig. 9.

Next, we examined the top face of the rendering-model (Fig. 9) for surface homogeneity. When transforming the ToF-SIMS measurements into a heat-map of the trityl$^+$-signals distributions, the solution based (DMF) coupling reactions resulted into very uniform signals, whereas the particle-based immobilization of Fmoc-Cys(Trt)-OPfp showed a leopard-like distribution of the coupled amino acid (Fig. 10). Clearly, using the particle matrix material as a medium for coupling the cysteine derivative did not result into homogeneous coverage of the synthesis surface. Thus, repetitive coupling should improve the homogeneity.

Due to its wetting properties, the viscous matrix material favors isle-like formations on the PEGMA surface (contact angle: $\Theta = 41.3^\circ$ at 160 °C). With respect to the high-density peptide microarray synthesis, this very same effect is highly desirable as it prevents adjacent amino acid spots from blending into one another. Therefore, in contrast to the SPOT-Technique, where solubilized amino acids are spotted onto the substrate, the particle-based approach allows for very high-density *in situ* peptide arrays.

4. Conclusion

Particle-based combinatorial coupling of amino acid building blocks results into peptide arrays of unrivalled density [13,14,18]. It is much easier to scale down the size of peptide spots by using solid materials when compared to liquids that tend to spread on the surface and to operate. Rivalling lithographic methods [10,12] suffer from another drawback when compared to the printing techniques: the 20 different amino acid building blocks have to be coupled one after another to the surface to complete a single layer of amino acids ($10 \times 20 = 200$ coupling steps for an array of decamer peptides), leading to an intolerable amount of unwanted side reactions. In order to better understand the particle-based solid phase peptide synthesis on polymer films we scrutinized the coupling behavior of amino acid derivatives to polymer films by comparing coupling results from microparticles to solution-based amino acid coupling (as used in the SPOT-synthesis). The presented ToF-SIMS depth profiling results should lead to optimized synthesis strategies: (1) clearly, the viscous particle matrix material can only penetrate about 60 nm into the PEGMA film, which advocates for the use of thinner PEGMA layers. Less dense, and therefore, less protein resistant PEGMA layers are better suited for antibody-based bioassays, because they do not block the antibodies from accessing the surface [40]. (2) In order to achieve a homogenous coupling of the amino acid building blocks (see Fig. 10), particles with a lower glass transition temperature are preferred. These modified particle and surface parameters should result in better peptide array quality and, thereby, improve the quality of various biotechnological assays that employ high density peptide arrays. We hereby showed that ToF-SIMS requires careful control of several analytical parameters and can indeed serve as a tool to analyze a highly complex organic, chemically modified surface in 3D and in nanoscale dimensions.

Acknowledgments

The authors gratefully acknowledge the support by the KNMF and the financial support by the ERC St Grant no. 277863, the HRJRG grant no. 316, the Carl-Zeiss-Stiftung, the BMBF KATMETHAN grant no. 03EK3030A, the EU FP7 PEPDIODE (grant no. 256672), and the EU FP7 TARGETBINDER (grant no. 278403).

Appendix A. Supplementary data

Supplementary data associated with this article can be found, in the online version, at http://dx.doi.org/10.1016/j.apsusc.2015.10.223.

References

[1] R. Frank, Spot-synthesis: an easy technique for the positionally addressable, parallel chemical synthesis on a membrane support, Tetrahedron 48 (1992) 9217–9232.
[2] R. Frank, The SPOT-synthesis technique Synthetic peptide arrays on membrane supports-principles and applications, J. Immunol. Methods 267 (2002) 13–26.
[3] R.B. Merrifield, Solid phase peptide synthesis. I. The synthesis of a tetrapeptide, J. Am. Chem. Soc. 85 (1963) 2149–2154.
[4] INTAVIS Bioanalytical Instruments AG, Germany, http://www.intavis.com/.
[5] JPT Peptide Technologies, Germany, http://www.jpt.com/.
[6] R. Volkmer, Synthesis and application of peptide arrays: quo vadis SPOT technology, Chembiochem 10 (2009) 1431–1442.
[7] C. Katz, L. Levy-Beladev, S. Rotem-Bamberger, T. Rito, S.G. Rudiger, A. Friedler, Studying protein-protein interactions using peptide arrays, Chem. Soc. Rev. 40 (2011) 2131–2145.
[8] A. Dikmans, U. Beutling, E. Schmeisser, S. Thiele, R. Frank, SC2: a novel process for manufacturing multipurpose high-density chemical microarrays, QSAR Comb. Sci. 25 (2006) 1069–1080.
[9] F. Breitling, A. Nesterov, V. Stadler, T. Felgenhauer, F.R. Bischoff, High-density peptide arrays, Mol. BioSyst. 5 (2009) 224–234.
[10] S.P.A. Fodor, J.L. Read, M.C. Pirrung, L. Stryer, A.T. Lu, D. Solas, Light-directed, spatially addressable parallel chemical synthesis, Science 251 (1991) 767–773.
[11] J.W. Jacobs, S.P.A. Fodor, Combinatorial chemistry-applications of light directed chemical synthesis, Trends Biotechnol. 12 (1994) 19–26.
[12] J.P. Pellois, X. Zhou, O. Srivannavit, T. Zhou, E. Gulari, X. Gao, Individually addressable parallel peptide synthesis on microchips, Nat. Biotechnol. 20 (2002) 922–926.
[13] M. Beyer, A. Nesterov, I. Block, K. Konig, T. Felgenhauer, S. Fernandez, K. Leibe, G. Torralba, M. Hausmann, U. Trunk, V. Lindenstruth, F.R. Bischoff, V. Stadler,

F. Breitling, Combinatorial synthesis of peptide arrays onto a microchip, Science 318 (2007) 1888.
[14] V. Stadler, T. Felgenhauer, M. Beyer, S. Fernandez, K. Leibe, S. Guttler, M. Groning, K. Konig, G. Torralba, M. Hausmann, V. Lindenstruth, A. Nesterov, I. Block, R. Pipkorn, A. Poustka, F.R. Bischoff, F. Breitling, Combinatorial synthesis of peptide arrays with a laser printer, Angew. Chem. Int. Edit. 47 (2008) 7132–7135.
[15] M. Beyer, Entwicklung und Anwendung neuartiger Trägeroberflächen zur kombinatorischen Peptidsynthese mit Aminosäure-Tonerpartikeln, in Physical-Chemical Institute, Ruperto-Carola University, Heidelberg, 2005, PhD Thesis.
[16] M. Beyer, T. Felgenhauer, F.R. Bischoff, F. Breitling, V. Stadler, A novel glass slide-based peptide array support with high functionality resisting non-specific protein adsorption, Biomaterials 27 (2006) 3505–3514.
[17] F. Maerkle, Laserbasierte Verfahren zur Herstellung hochdichter Peptidarrays, Karlsruhe Institute of Technology, 2014, PhD Thesis.
[18] F. Maerkle, F.F. Loeffler, S. Schillo, T. Foertsch, B. Muenster, J. Striffler, C. Schirwitz, F.R. Bischoff, F. Breitling, A. Nesterov-Mueller, High-density peptide arrays with combinatorial laser fusing, Adv. Mater. 26 (2014) 3730–3734.
[19] A. Benninghoven, Chemische Analyse von anorganischen und organischen Oberflächen und von dünnen Schichten mit der statischen Flugzeit-Sekundärionen-Massenspektrometrie (TOF-SIMS), Angew Chem. 106 (1994) 1075–1096.
[20] A. Delcorte, Fundamentals of organic SIMS: insights from experiments and models, in: J. Vickermann, D. Briggs (Eds.), TOF-SIMS: Materials Analysis by Mass Spectrometry, 2nd ed., IM publications, Chichester, UK, 2013, ISBN: 978-1-906715-17-5.
[21] S.J. Valenty, J.J. Chera, D.R. Olson, K.K. Webb, G.A. Smith, W. Katz, Multitechnique depth profiling of small molecules in polymeric matrices, J. Am. Chem. Soc. 106 (1984) 6155–6161.
[22] J.S. Fletcher, J.C. Vickerman, A new SIMS paradigm for 2D and 3D molecular imaging of bio-systems, Anal. Bioanal. Chem. 396 (2010) 95–104.
[23] J. Cheng, N. Winogard, Depth profiling of peptide films with TOF-SIMS and a C60 probe, Anal. Chem. 77 (2005) 3651–3659.
[24] G. Gillen, S. Roberson, Preliminary evaluation of an SF5 + polyatomic primary ion beam for analysis of organic thin films by secondary ion mass spectrometry, Rapid. Commun. Mass. Spectrom. 12 (1998) 1303–1312.
[25] A.G. Shard, I.S. Gilmore, A. Wucher, Molecular depth profiling, in: J. Vickermann, D. Briggs (Eds.), TOF-SIMS: Materials Analysis by Mass Spectrometry, 2nd ed., IM publications, Chichester, UK, 2013, ISBN: 978-1-906715-17-5.
[26] A.G. Shard, R. Havelund, S.J. Spencer, I.S. Gilmore, M.R. Alexander, T.B. Angerer, S. Aoyagi, J.-P. Barnes, A. Benayad, A. Bernasik, G. Ceccone, J.D.P. Counsell, C. Deeks, J.S. Fletcher, D.J. Graham, C. Heuser, T.G. Lee, C. Marie, M.M. Marzec, G. Mishra, D. Rading, O. Renault, D.J. Scurr, H.K. Shon, V. Spampinato, H. Tian, F. Wang, N. Winograd, K. Wu, A. Wucher, Y. Zhou, Z. Zhu, Measuring compositions in organic depth profiling: results from a VAMAS interlaboratory study, J. Phys. Chem. B 119 (2015) 10784–10797.
[27] C.M. Mahoney, Cluster secondary ion mass spectrometry of polymers and related materials, Mass. Spec. Rev. 29 (2010) 247–293.
[28] A.J. Taylor, D.J. Graham, D.G. Castner, Reconstructing accurate ToF-SIMS depth profiles for organic materials with differential sputter rates, Analyst 140 (2015) 6005–6014.
[29] K. Shen, A. Wucher, N. Winograd, Molecular depth profiling with argon gas cluster ion beams, J. Phys. Chem. C 119 (2015) 15316–15324.
[30] A.G. Shard, M.P. Seah, Depth resolution and inhomogeneity of the sputtering dose with sample rotation and ion beam rastering, Surf. Interface Anal. 43 (2011) 1430–1435.
[31] L. Bernard, J. Heier, W. Paul, H.J. Hug, The SFM/ToF-SIMS combination for advanced chemically-resolved analysis at the nanoscale, Nucl. Instrum. Methods Phys. Res., Sect. B 339 (2014) 85–90.
[32] P. Sjövall, D. Rading, S. Ray, L. Yang, A.G. Shard, Sample cooling or rotation improves C60 organic depth profiles of multilayered reference samples: results from a VAMAS interlaboratory study, J. Phys. Chem. B 114 (2010) 769–774.
[33] A. Zalar, Improved depth resolution by sample rotation during Auger electron spectroscopy depth profiling, Thin Solid Films 124 (1985) 223–230.
[34] J.-S. Wang, K. Matyjaszewski, Controlled/"Living" radical polymerization. Atom transfer radical polymerization in the presence of transition-metal complexes, J. Am. Chem. Soc. 117 (1995) 5614–5615.
[35] W.A. Braunecker, K. Matyjaszewski, Controlled/living radical polymerization: features, developments and perspectives, Prog. Polym. Sci. 32 (2007) 93–146.
[36] W. Feng, R. Chen, J.L. Brash, S. Zhu, Surface-initiated atom transfer radical polymerization of oligo(ethylene glycol)methacrylate: effect of solvent on graft density, Macromol. Rapid. Comm. 26 (2005) 1383–1388.
[37] B. Czerwinski, L. Rzeznik, K. Stachura, R. Paruch, B.J. Garrison, Z. Postawa, Applications of fullerene beams in analysis of thin layers, Vacuum 82 (2008) 1120–1123.
[38] I.S. Gilmore, SIMS of organics – advances in 2D and 3D imaging and future outlook, J. Vac. Sci. Technol. A 31 (2013) 050819.
[39] J.S. Fletcher, Latest applications of 3D ToF-SIMS bio-imaging, Biointerphases 10 (2015) 018902.
[40] V. Stadler, R. Kirmse, M. Beyer, F. Breitling, T. Ludwig, F.R. Bischoff, PEGMA/MMA copolymer graftings: Generation, protein resistance, and a hydrophobic domain, Langmuir 24 (2008) 8151–8157.